

# Enhancing hydrologic LiDAR digital elevation models: Bridging hydrographic gaps at fine scales

Di Wu<sup>1</sup> | Ruopu Li<sup>2</sup> | Michael Edidem<sup>2</sup> | Guangxing Wang<sup>2</sup>

<sup>1</sup>Department of Geography, University of Colorado, Boulder, Colorado, USA

<sup>2</sup>School of Earth Systems and Sustainability, Southern Illinois University, Carbondale, Illinois, USA

## Correspondence

Ruopu Li, School of Earth Systems and Sustainability, Southern Illinois University, Carbondale, IL, USA.  
Email: [ruopu.li@siu.edu](mailto:ruopu.li@siu.edu)

## Funding information

National Science Foundation, Grant/  
Award Number: 1951741

## Abstract

High-resolution digital elevation models (HRDEMs), derived from LiDAR, are widely used for mapping hydrographic details in flat terrains. However, artificial flow barriers, particularly from roads, elevate terrain and prematurely end flowlines. Drainage barrier processing (DBP), such as HRDEM excavation, is employed to address this issue. However, there is a gap in quantitatively assessing the impact of DBP on HRDEM-derived flowlines, especially at finer scales. This study fills that gap by quantitatively assessing how DBP improves flowline quality at finer scales. We evaluated HRDEM-derived flowlines that were generated using different flow direction algorithms, developing a framework to measure the effects of flow barrier removal. The results show that the primary factor influencing flowline quality is the presence of flow accumulation artifacts. Quality issues also stem from differences between natural and artificial flow paths, unrealistic flowlines in flat areas, complex canal networks, and ephemeral drainage ways. Notably, the improvement achieved by DBP is demonstrated to be more than 6%, showcasing its efficacy in reducing the impact of flow barriers on hydrologic connectivity.

## KEY WORDS

LiDAR, DEM, hydrography, hydrologic connectivity, National Hydrography Dataset

## 1 | INTRODUCTION AND BACKGROUND

The pivotal role of hydrologic connectivity in understanding hydro-geomorphological processes and managing environmental resources necessitates the development of flowline networks at appropriate scales. Stream flowline datasets with high spatial accuracy at a regional scale can facilitate a range of environmental applications, including watershed management (Heathcote, 2009), wetland dynamics (Jenkins & Frazier, 2010), sediment transportation (Carrivick et al., 2010), and gully erosion measurement (Hout et al., 2020). While flowlines at coarser spatial scales are more effective in representing hydrologic connectivity at national and global scales (Fekete et al., 2001), finer-scale networks are required for accurately representing individual or small, localized basins and tributaries.

The National Hydrography Dataset (NHD) is a widely used GIS data source for representing comprehensive surface water features (e.g., lakes, streams, rivers, and canals) in the United States (U.S.) (Buttenfield et al., 2011). This dataset is available at two scales, 1:24,000 (high-resolution version) and 1:100,000 (medium-resolution version), catering to diverse mapping needs. Enhancements to the NHD, such as NHDPlus and NHDPlus HR, incorporate features from the 10-meter National Elevation Dataset (currently part of the U.S. Geological Survey's 3DEP program) and the National Watershed Boundary Dataset (WBD). These features include improved networking, elevation-based catchment

## Research Impact Statement

A new study develops a method and metrics for evaluating the effects of drainage barriers on the accuracy of the modeled flowlines using LiDAR DEMs.

areas, flow surfaces, and value-added attributes that enhance stream-network navigation, analysis, and visualization (Mckay et al., 2014). The NHD and its enhancement have been widely utilized across various environmental and ecological applications, such as pollution control, the management of aquatic biota, and hydrologic analysis (Anderson-Tarver et al., 2012; Evenson et al., 2018; Fesemeyer et al., 2021; Figary et al., 2021; Huang & Frimpong, 2016; Mukhopadhyay et al., 2020; Simley, 2008).

While the NHD effectively portrays surface water features at the national scale, it is subject to limitations such as map-to-map inconsistencies, errors in the transformation of the data from maps to digital datasets, and limited feature density (Simley, 2008). The irregular and inconsistent update cycle of 1:24,000-scale NHD dataset has resulted in varying data quality across different watersheds (Anderson-Tarver et al., 2011). Thus, efforts to integrate user-generated updates into the NHD have been proposed to address its data quality issues. The U.S. Geological Survey (USGS) has developed "Elevation-Derived Hydrography Specifications" to refine the NHD, enhancing water-related data discovery and sharing. Despite NHD's broad applications, there is an increasing need for data compiled at even finer scales, such as 1:4800, a substantial enhancement compared to the current 1:24,000 and 1:100,000 scales (Simley, 2008; Strager, 2019; Thompson et al., 2018; Wilmer, 2010). However, drainage patterns at such high scales are inconsistently available, exhibiting varied formats and quality across individual mapping projects.

Light detection and ranging (LiDAR), with its high spatial resolution and accuracy, has been proven to help improve the representation of surface water features at local scales. The high-resolution digital elevation models (HRDEMs) that are produced from LiDAR source data have been widely used in hydrologic modeling. Li and Wong (2010) proved that HRDEM with 2-m resolution outperforms 10-m and 30-m National Elevation Dataset (NED) and Shuttle Radar Topography Mission (SRTM) data in extracting river networks when the cell sizes in comparing extracted rivers are relatively small. Lang et al. (2012) found that the NHD products tend to underestimate the percent area and total number of wetlands, and stream datasets derived from semi-automated and automated interpretation of 1-m HRDEMs exhibit higher accuracy than NHDPlus and NHDPlus HR. Steinke and Ogden (2013) claimed that the utilization of HRDEMs and other high-accuracy measurements enhances the performance of hydrologic modeling in channels, especially in areas characterized by low slopes. Poppenga et al. (2013) utilized surface channels derived from 3-m HRDEMs to improve hydrography change detection, suggesting a viable approach for updating the NHD flowlines.

Despite high resolution and extraordinary accuracy, HRDEMs presents unique challenges in hydrologic applications. Yang and Chu (2013) demonstrated that HRDEMs can cause the underestimation and segmentation of hydrologic connectivity. Barber and Shortridge (2005) found that HRDEMs can misrepresent flow barriers like bridges and graded roadbeds over culverts, resulting in large sinks, false watershed boundaries, and even non-existent sub-watersheds. These barriers, represented as an elevated road surface or a bridge above a waterway channel in HRDEMs, often cause inaccuracies in modeled drainage flowlines, such as incorrect crossing points or sudden termination (Bhadra et al., 2021; Li et al., 2013; Sofia et al., 2014). To address these limitations, HRDEM excavation has been widely employed to generate a hydrologic version of the HRDEM, mitigating the segmentation of hydrologic connectivity and improving the spatial accuracy of HRDEM-derived flowlines (Aristizabal et al., 2018; Li et al., 2013; Lindsay & Dhun, 2015). However, there remains a gap in quantitatively assessing the extent to which HRDEM excavation can enhance the quality of DEM-derived flowlines, particularly at a finer scale.

This study aims to quantitatively assess how the processing of flow barriers in HRDEMs enhances the quality of flowlines at finer scales. The method involves utilizing HRDEM excavation for breaching flow barriers in HRDEM prior to simulating elevation-derived flowlines. As a departure from the commonly used metric "offset distance" that was only applicable to point locations (Bhadra et al., 2021; James et al., 2012), we assess the accuracy of flowlines arising from the removal of flow barriers in HRDEM using the Coefficient of Line Correspondence (CLC). This research contributes to the state of the art by (1) developing an assessment framework for quantifying the effects of flow barriers' removal on the LiDAR-derived flowline features, and (2) evaluating the quality of LiDAR-derived flowline in a comparison with the NHD and ground truth data.

## 2 | STUDY AREAS AND DATASETS

### 2.1 | Study area

The study area in this chapter is Flat Creek Watershed, a sub-watershed in West Fork Big Blue Watershed, Nebraska (Figure 1). It is a predominantly agricultural watershed devoted to row crops, mainly corn, grain sorghum, and soybeans. Dense road networks segment the landscape over the study area, resulting in widespread flow barriers for the representation of drainage features.

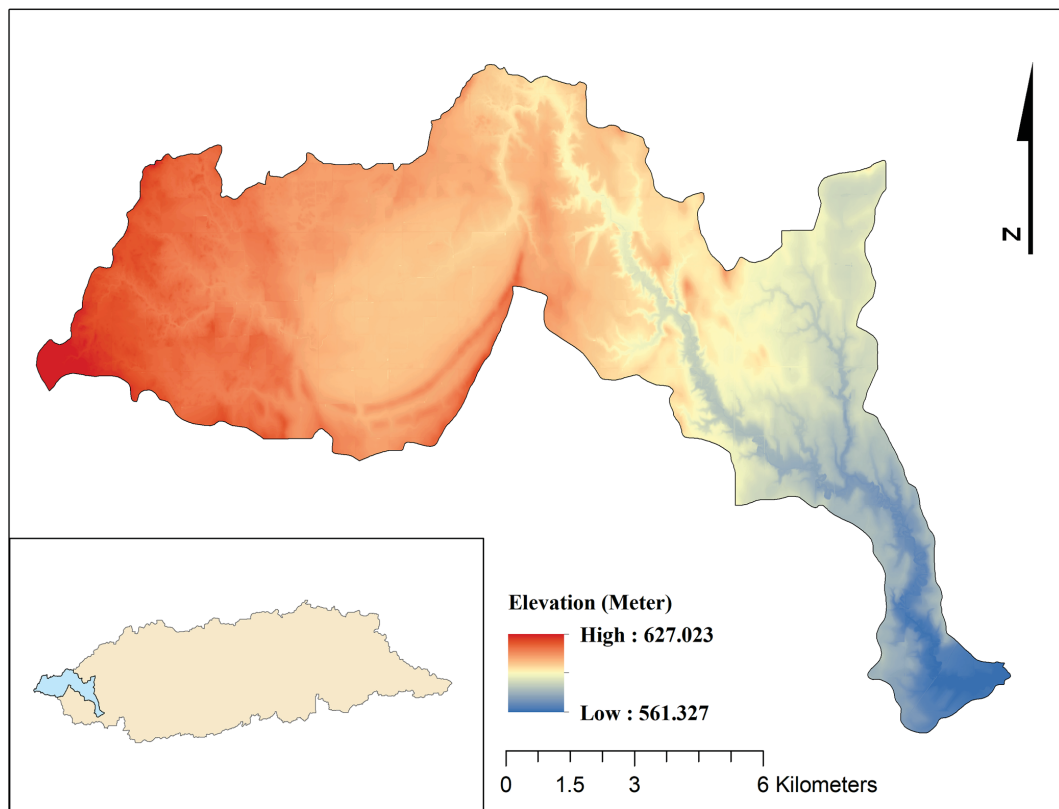


**FIGURE 1** Topography and locations of Flat Creek Watershed.

## 2.2 | Dataset

The sources of HRDEM and aerial orthophotos for the Flat Creek Watershed, Nebraska are listed in [Table 1](#). Color infrared aerial images from National Agriculture Imagery Program (NAIP) contain red, green, blue, and near-infrared bands, with 1-meter horizontal resolution, which are used as a base map to evaluate the results.

Ground truth was developed at a finer scale by correcting the 1:24,000-scale NHD flowlines from the USGS Hydrography Dataset Plus High Resolution (NHDPlus HR). Since the NHD falls short in satisfying the growing user demand for high-resolution and high-accuracy hydrography information (Poppenga et al., 2013; Simley, 2008), we conducted minor corrections of the current NHD data and then extended the NHD to the scale 1:12,000 by digitizing small stream segments manually using the HRDEM and the most recent (released in 2022) NAIP aerial images as base maps ([Figure 2](#)). This 'corrected' version of NHD was regarded as 'ground truth', serving as the benchmark for comparison and validation ([Figure 3](#)). To identify the optimal threshold for flowline accumulation, a set of channel initiation points were also digitized at the scale of 1:12,000. Manually digitized vector lines crossing through bridges and culverts were also utilized for DEM excavation.

## 3 | METHODOLOGY

The workflow is shown as [Figure 4](#). Based on digitized vector lines crossing the hydraulic structures, AGREE algorithm, the technique of DEM excavation, was employed to breach flow barriers in HRDEMs to generate modified DEM. Flow accumulation based on modified DEM was utilized to delineate the flowlines. By comparing the generated flowlines with corrected NHD 'benchmark', we evaluated the quality of DEM-derived flowlines on a finer scale.

### 3.1 | HRDEM preprocessing

To produce a consistent hydrologic connectivity dataset, a HRDEM should be modified by excavating the hydraulic drainage barriers to a lower elevation. Stream burning has been used widely to reduce the elevations within the existing channels, which ensures that the water will flow downstream along the channels (Lindsay, 2016). To apply stream burning for drainage barrier processing (DBP), we adopted the AGREE algorithm that allows a

**TABLE 1** Data sources for Flat Creek Watershed, Nebraska.

Data	Sources	Scale/resolution
DEM	Nebraska Department of Natural Resource	1.0m
Aerial orthophotos	USGS National Agriculture Imagery Program (NAIP)	1.0m
NHD	USGS	1:24,000


**FIGURE 2** An example of NHD update caused by terrain surface changes. An artificial ditch was constructed after NHD generated (left). In the right image, the red line represents the original NHD flowline, while the cyan line is the corrected NHD flowline.

smooth change of surface elevation. AGREE is designed by Hellweger (1997), which is a DEM reconditioning algorithm to adjust the surface elevation of the DEM to be consistent with a stream. By providing a linear fit to the grid cells from the edge of the buffer zone to the cell locations of the raster streams, AGREE algorithm drops the elevation of the DEM cells corresponding to user-defined buffer distance around the stream flowlines, avoiding the abrupt jumps in elevation between stream and non-stream cells and ensuring straight flow paths between the network cells and the buffer border cells. This process will effectively remove the 'digital dams' caused by road embankments, culverts, or bridges (Bhadra et al., 2021; Li et al., 2013; Saunders, 2000). In this study, the AGREE was conducted in ArcGIS 10.8 by using DEM reconditioning in ArcHydro Toolbox. Manually digitalized vector line segments, which indicate drainage crossing locations, were used for the DBP. Along these vector lines, a channel with specified width and depth is excavated by the AGREE algorithm. Two user-specified elevation offset values are accepted by AGREE, a "smooth" value for integrating the vector stream network into the DEM, and a "sharp" value for integrating the smoothed buffer zone into the DEM. In our study, we selected buffer 5 m, smooth drop 5 m, and sharp drop 1 m as the parameters of the algorithm, which is consistent with the general river geomorphology in the study area.

Depressions, also referred to as sinks or pits, are areas with low elevation in DEMs that are surrounded by higher terrain and have no outlet (Barnes et al., 2014a). Since the depressions could interfere with the flow routing, depression-free DEMs are commonly required in standard DEM-based hydrological analysis. Depression filling removes the depressions by raising their elevation to the point where the water drains off the edge of the domain (Tarboton & Mohammed, 2013). We implemented Pit Remove Tools in Terrain Analysis Using Digital Elevation Models (TauDEM v5.3) to fill all depressions in the study area.

### 3.2 | Flowlines delineation

Commonly there are four key steps for modeling stream flowlines based on preprocessed DEMs, including flow direction calculation, flow accumulation, stream definition by thresholds, and vector-based stream flowlines construction. Depression processing ensures the water can flow downstream without interruption, based on which flow direction and flow accumulation algorithms are applied to DEM (Jenson & Domingue, 1988). There are two types of flow direction algorithms, Single Flow Direction (SFD) and Multiple Flow Direction (MFD). The SFD algorithm assumes that the water from one cell should flow into only one neighboring cell that has the lowest elevation (Bhadra et al., 2021).

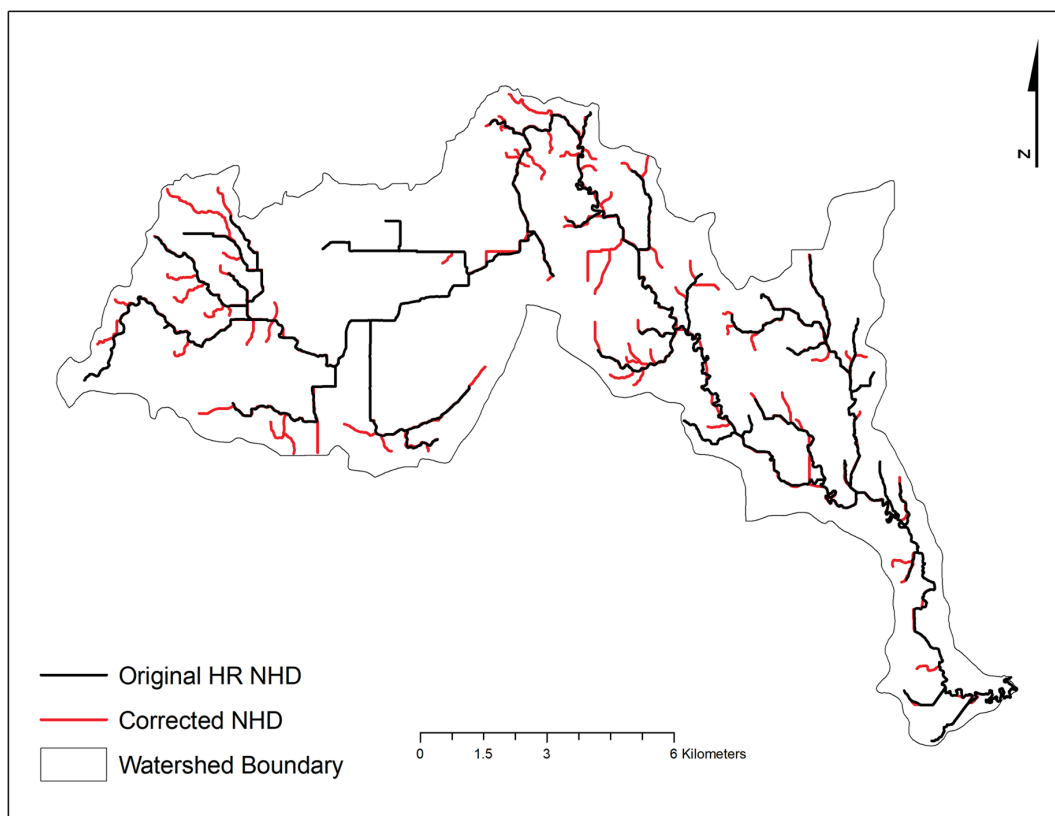


**FIGURE 3** Comparison between original HR NHD (black lines) and corrected NHD ground truth (red lines).

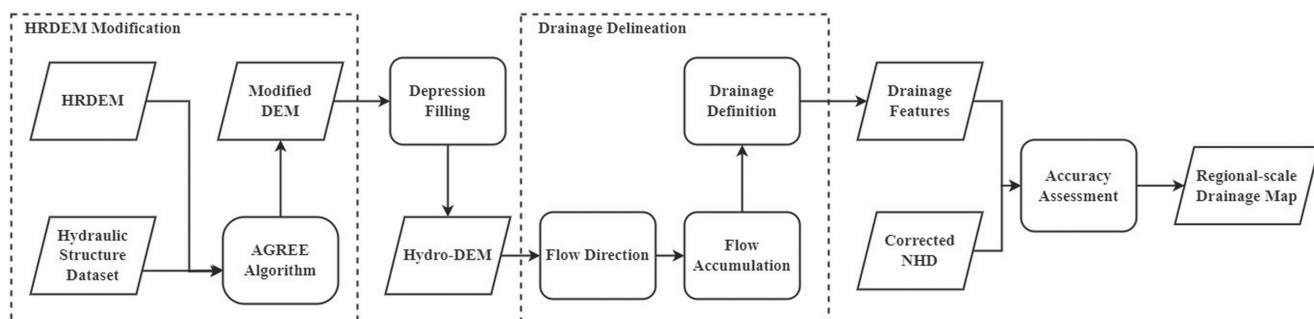


**FIGURE 4** Workflow for hydrologic modeling based on the HRDEMs.

As its idea of the steepest descent direction is easy to implement, SFD algorithms have been widely adopted by GIS software packages, which are suitable for modeling convergent flow (Qin et al., 2007). MFD algorithms allow continuous flow angles, assuming that the flow from a DEM cell could drain into more than one downslope neighboring cell (Qin et al., 2007). The fraction of flow draining among downslope neighboring cells is determined based on slope gradient (Quinn et al., 1991). Compared with SFD, MFD could compute contributing areas more accurately on divergent hillslopes. To compare the performance of these two types of flow direction algorithms, Deterministic Eight (D8) from SFD and Deterministic Infinity (D-Infinity) from MFD will be used in this study.

### 3.2.1 | Flow direction algorithms

D8 is one of the most popular SFD algorithms. The major idea of D8 is to track the flow from each pixel to one of its eight neighbor pixels (O'Callaghan & Mark, 1984; Wang et al., 2011). As a powerful algorithm, it could assign reasonable flow directions even in very complex and ambiguous situations. D-Infinity algorithm (Tarboton, 1997) assumes that water flows down one or two cells by partitioning the flow between the two cells nearest to the steepest slope direction (Yang et al., 2015). The flow direction is a vector along the direction of the steepest downward slope on the eight triangular facets formed in a  $3 \times 3$  grid cell window centered on the grid cell of interest.

### 3.2.2 | Flow accumulation threshold (FAT)

The flow accumulation threshold (FAT) is a parameter that could directly affect the structure and density of extracted river networks from DEMs (Ozulu & Gökgöz, 2018). As a user-defined parameter, a too-large FAT would omit useful details of river networks, while a too-small FAT would lead to a highly dense river network dominated by pseudo flowlines (Zhang et al., 2021). The traditional method to determine a stream threshold was trial and error based on visual interpretation, which is often subjective and time-consuming. The identification of channel initiations, which could determine the essential topology and morphometric characteristics of downstream, is critical for the extraction of a drainage network from DEMs. Since the positioning of the ends of drainage networks fluctuates with the threshold value, a method that should be more objective and accurate than an arbitrary visual judgment is needed. Lin et al. (2006) developed the fitness index, a quantitative analysis method, which calculates the channel initiation error length between the observed and calculated values to determine the reasonable stream threshold. The fitness index Equation is shown in (1),

$$F = \frac{\sum_{s=1}^n (L_i)_s + \sum_{s=1}^n (L_r)_s}{L_T}, \quad (1)$$

where  $L_i$  is the insufficient stream length,  $L_r$  is the redundant stream length, and  $L_T$  is the total stream length extracted from aerial photographs. As we generated a “ground truth” stream under a constant scale, the formula of the fitness index could be simplified as Equation (2), where the FAT which minimizes the value of  $F$  could be regarded as the reasonable threshold,

$$F = \sum_{s=1}^n (L_i)_s + \sum_{s=1}^n (L_r)_s. \quad (2)$$

### 3.3 | Flowline comparison and accuracy assessment

The coefficient of line correspondence (CLC) has been developed by Stanislawski (2009), which is a ratio being used to compare how two sets of lines that represent similar features on the ground match each other. In the equation of CLC (shown as Equation (3)),  $M$  is the sum of the lengths of matching benchmark lines, omission error  $O$  is the sum of the length of benchmark lines that are omitted from the generated lines, and commission error  $C$  is the sum of the length of lines in the generated data that do not have a match in the benchmark. The higher the CLC, the better two sets of lines match spatially. A high CLC value indicates a substantial degree of agreement between two sets of lines,

$$CLC = \frac{M}{M + O + C}. \quad (3)$$

The proportions of commission errors are calculated by Equation (4),

$$P_c = \frac{C}{M + O + C}. \quad (4)$$

The proportions of omission errors are calculated by Equation (5),

$$P_O = \frac{O}{M + O + C}. \quad (5)$$

We generated buffers around the modeled and ground truth flow network features to assess omission and commission errors respectively. Omission errors were defined as the flowlines in the ‘ground truth’ benchmark network that fall mostly outside the buffer of the modeled flowlines, while the commission errors were estimated as the modeled flowlines which mostly fall outside the buffer of ground truth flowlines. In this study, the buffer size was set as 33.33 feet (around 10.2 m), following the National Map Accuracy Standard (NMAS) for 1:12,000-scale maps (Thomas et al., 2009).

## 4 | RESULTS

### 4.1 | D8 flowlines derived from HRDEM with DBP

#### 4.1.1 | FAT for stream delineation

Based on the D8 algorithm, the drainage networks were delineated by using various FATs. The FAT increases starting from 10,000 with a step of 10,000. The relationship between the fitness index and FAT is shown in Figure 5. With the FAT increases, the stream network density

decreases gradually, but the fitness index exhibits a U-shape trend. The FAT corresponding to the minimal fitness index is 40,000, which was selected as the optimal threshold for defining stream channels based on flow accumulation.

#### 4.1.2 | D8 drainage network

The modeled flowlines are shown in [Figure 6](#). The flowlines modeled using the excavated HRDEM are composed of natural streams, artificial canals and ditches, and the unrealistic parallels patterns. Based on the Elevation-derived Hydrography—Representation,

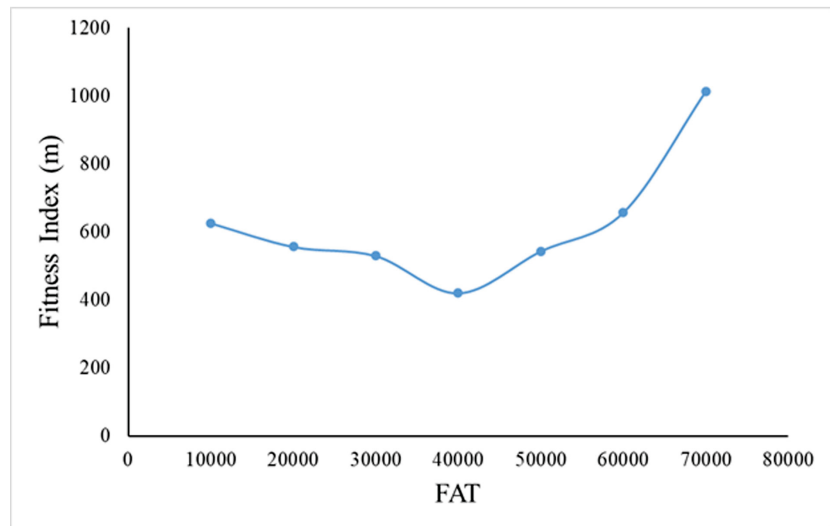


**FIGURE 5** The relationship between fitness index and FAT.

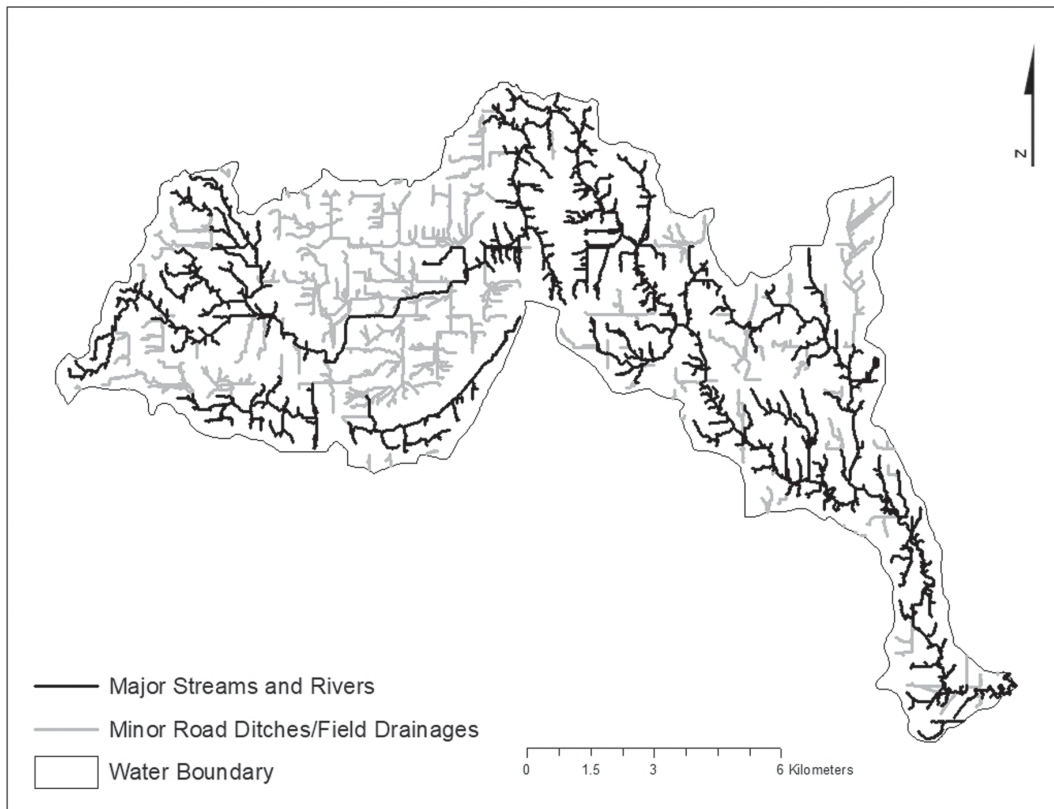


**FIGURE 6** D8-derived drainage network.

Extraction, attribution, and Delineation (READ) Rules (Archuleta & Terziotti, 2020) and elevation-derived hydrography acquisition specifications (Terziotti & Archuleta, 2020), a canal/ditch that does not provide network connectivity, is located in agricultural fields draining to another hydrologic feature, or is isolated should not be captured to avoid overcollection. Thus, we only focus on those streams, which are either flowing water channels with visible edge of the banks or the canals that connect different drainage lines (Archuleta & Terziotti, 2020). To evaluate the quality of the modeled D8 flowlines derived from the excavated HRDEM, we use the corrected NHD as the “ground truth” benchmark and the CLC as the quality metric. The comparison between the D8-modeled drainage lines and benchmark flowlines (1:12,000) is shown in Figure 7. Compared with the corrected NHD benchmark, the modeled drainage lines contain substantial flow accumulation artifacts that do not align with the corrected NHD. In the upstream area, a few branches disconnect from the primary flowlines because of the difficulty in determining the connectivity patterns. Further details will be addressed in the following section.

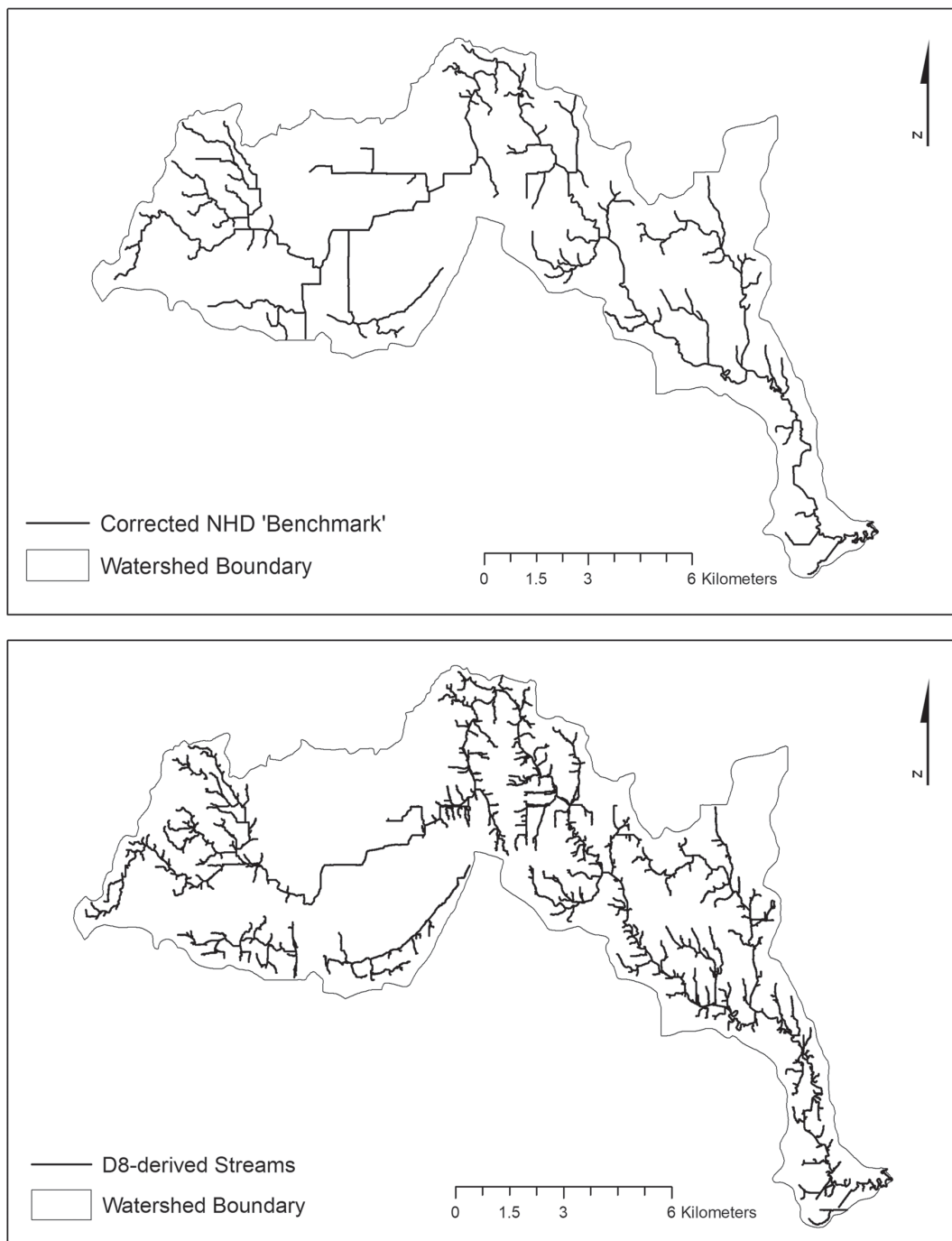


**FIGURE 7** The comparison between benchmark flowlines (upper) and D8-derived stream network (lower) at scale 1:12,000.

The CLC results are in [Table 2](#). The results show that the similarity between D8-derived drainage and the NHD benchmark is 47.11%, with the proportions of commission errors 47.72% and proportions of omission errors 5.17%. The distribution of omission and commission errors are shown in [Figures 8 and 9](#).

#### 4.2 | D8 flowlines derived from HRDEM without DBP

To assess the improvement of hydrologic connectivity that results from HRDEM excavation, flow networks were derived using the HRDEM, which maintained the elevation at drainage structures. The streams/rivers in D8-derived flowlines without DBP were then compared with the corrected NHD at a scale of 1:12,000. [Figures 10 and 11](#) illustrate the omission and commission errors observed in this comparison. Additionally, the CLC results, comparing the D8 flowline without HRDEM excavation against the corrected NHD “benchmark,” are presented in [Table 3](#). The CLC for flowlines derived from HRDEM without excavation and corrected NHD ‘ground truth’ is 40.59%, which is 6.52% lower than flowlines derived from the excavated HRDEM. The proportion of commission errors is 50.49% and the proportion of omission errors is 8.92%, which increased by 2.77% and 3.75% respectively compared with flowlines derived from the excavated HRDEM.

#### 4.3 | D-infinity flowlines derived from HRDEM

To explore the impact of flow direction algorithms on flowline generation, flowlines were produced using the D-Infinity algorithm with a FAT of 40,000. To evaluate the similarity between the flowlines generated by the D-Infinity algorithm and those created using the D8 algorithm,

**TABLE 2** CLC results for D8-derived streams with a FAT of 40,000 and a scale of 1: 12,000.

M (meter)	O (meter)	C (meter)	CLC	$P_O$	$P_c$
134,587	14,770	136,348	0.4711	0.0517	0.4772

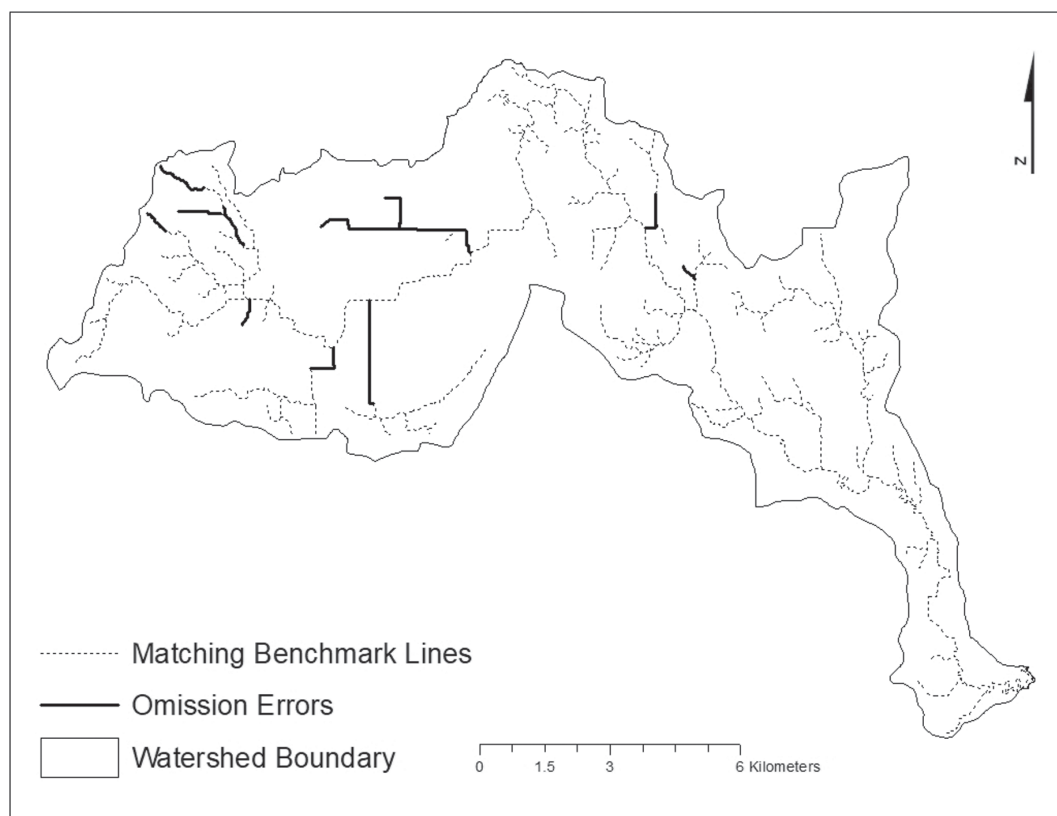


**FIGURE 8** Omission errors on benchmark lines when compared with D8-derived streams.

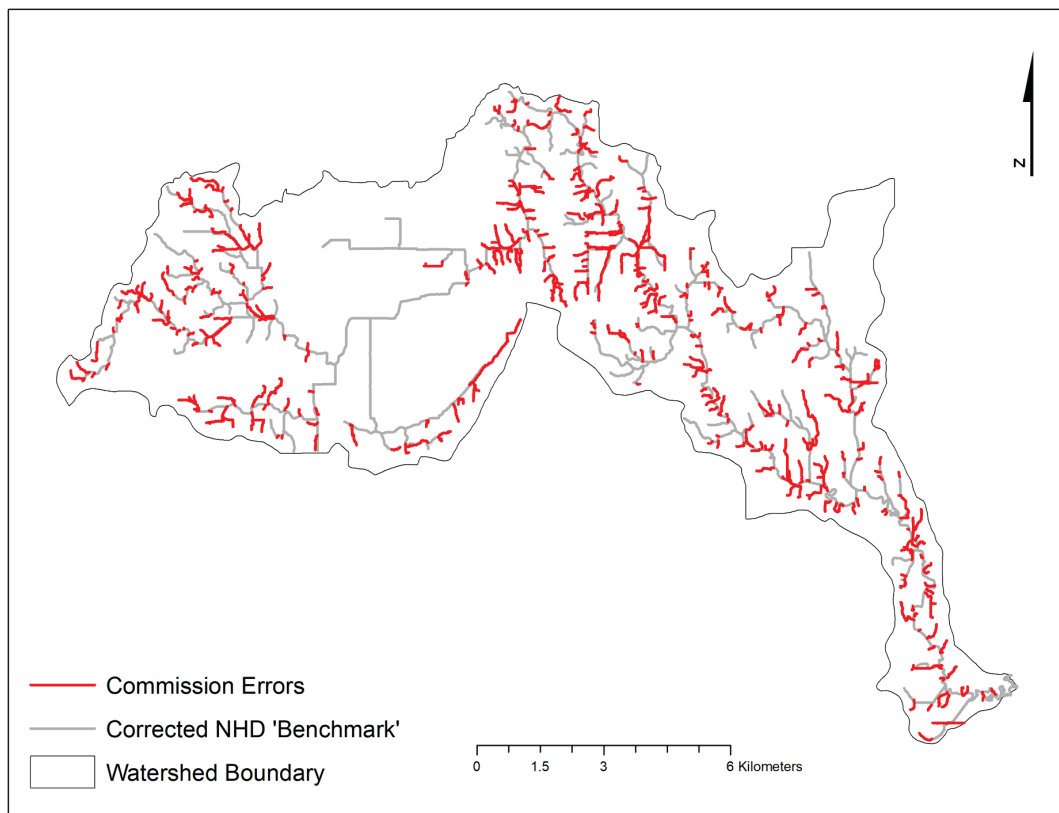


FIGURE 9 Commission errors from D8-derived streams.

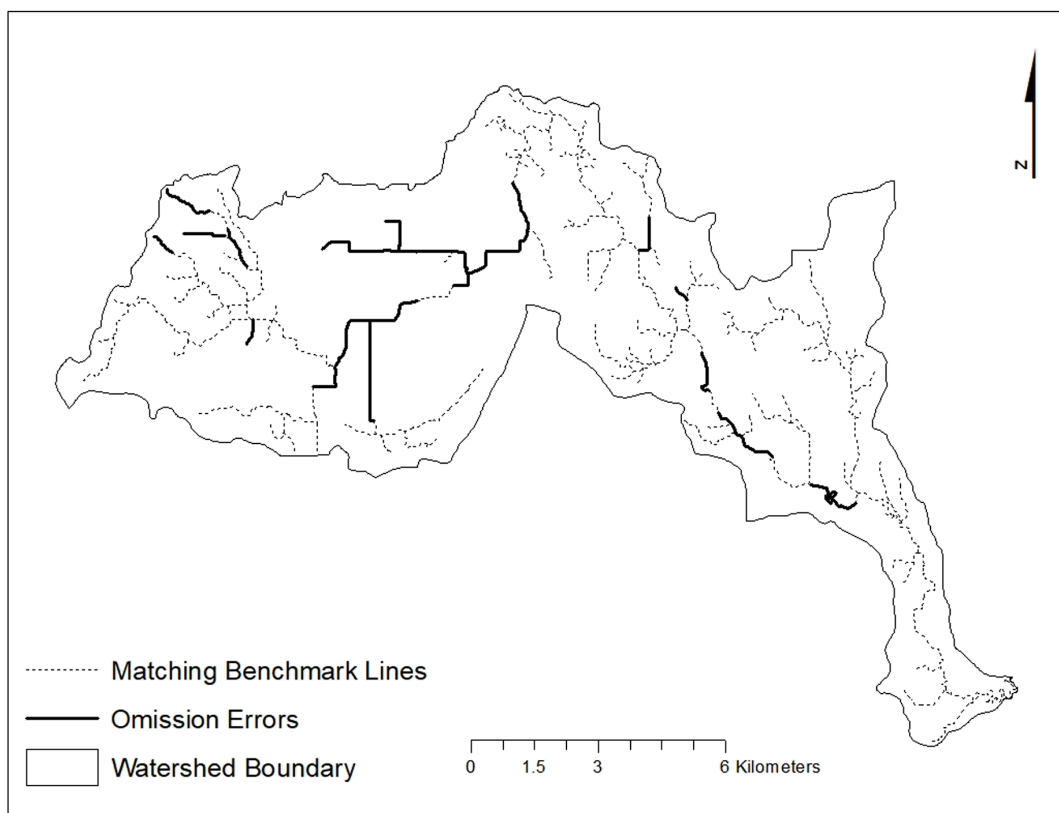
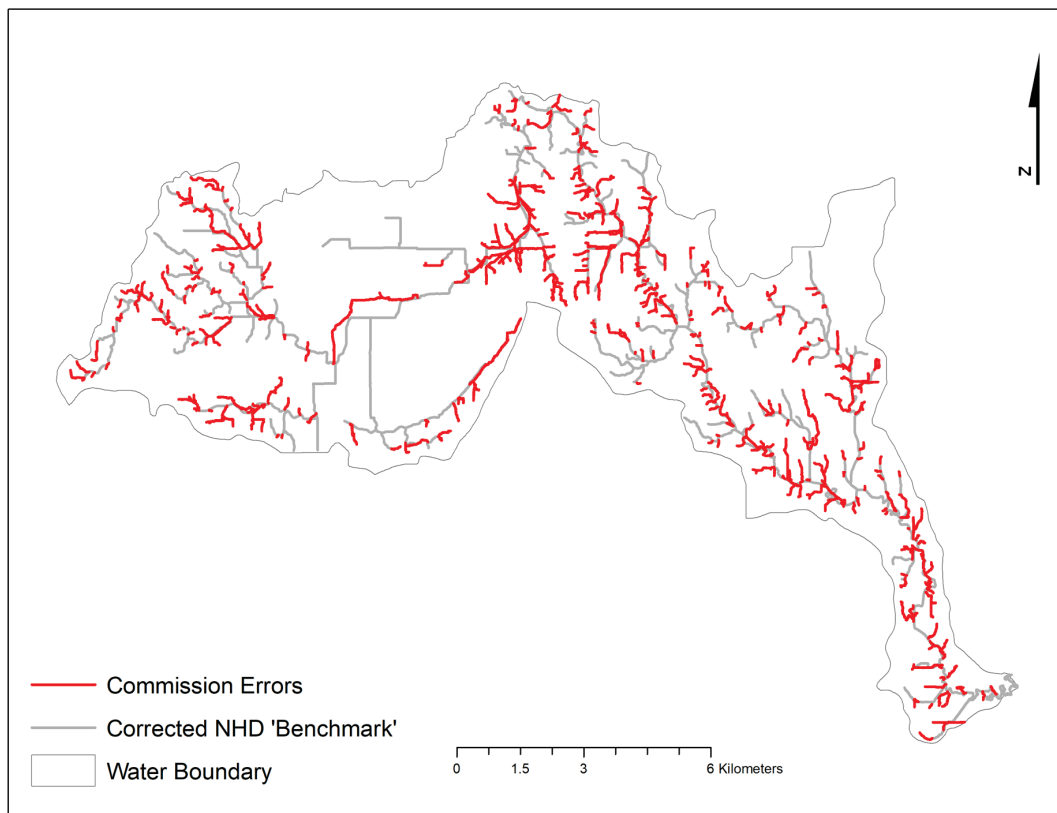


FIGURE 10 Omission errors on benchmark lines when compared with D8-derived streams without HRDEM excavation.



**FIGURE 11** Commission errors from D8-derived streams without HRDEM excavation.

**TABLE 3** CLC results for D8-derived streams based on the HRDEM without HRDEM excavation. The FAT is 40,000 with a scale of 1:12,000.

M (meter)	O (meter)	C (meter)	CLC	$P_O$	$P_c$
122,448	26,909	152,300	0.4059	0.0892	0.5049

the CLC was calculated, yielding a value of 0.9845. Since the high similarity between the flowlines generated by D8 and D-Infinity, we only discussed the difference between D8 flowlines and benchmark lines instead of D-Infinity.

## 5 | DISCUSSION

### 5.1 | Evaluation of fine-scale flowlines derived by the excavated HRDEM

The commission errors were mainly caused by flow accumulation and the use of a fixed FAT. Due to the fine elevation details captured by the HRDEM, it is common to include extra tributaries that may be missed in the corrected NHD benchmark. With the construction of civil infrastructures like roads, the difference between the natural topographic flowpaths and human-made flowpaths became a dilemma for flowlines simulation (Figure 12). In such a case, it was difficult to determine the actual ground truth without a field verification. Another factor contributing to the commission errors was the unrealistic flowline artifacts in flat areas (Figure 13). Apart from the naturally occurring flats like wetlands areas, the use of a depression-filling algorithm to generate a depression-less DEM also led to flat regions without any local elevation gradient. Flow directions in these areas were obscured by the elevation artifacts, resulting in local indeterministic flow directions and problematic parallel flow lines connecting stream segments (Zhang et al., 2017).

The omission errors in flowlines can be categorized into three types. The first type is associated with the canals that connect natural drainage lines (Figure 14a). According to the Elevation-Derived Hydrography READ Rules by Archuleta and Terziotti (2020), canals or ditches necessary for network connectivity should be included into the hydrography features. In agricultural areas, widespread

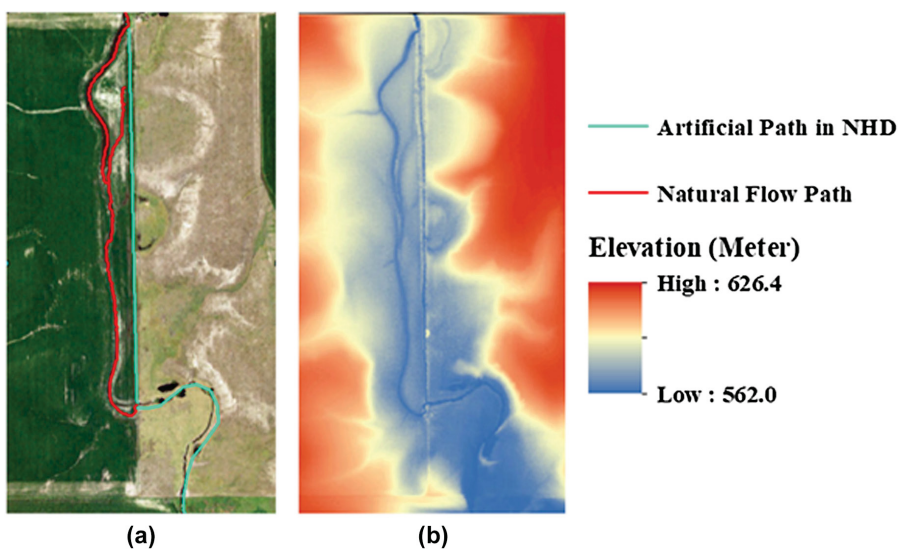


**FIGURE 12** An example of conflict between the natural topographic flow path and human-made flow path. (a) is the aerial photo where the cyan line is the human-made flow path (NHD), and red line is the natural topographic flow path; (b) is the HRDEM in the same area.

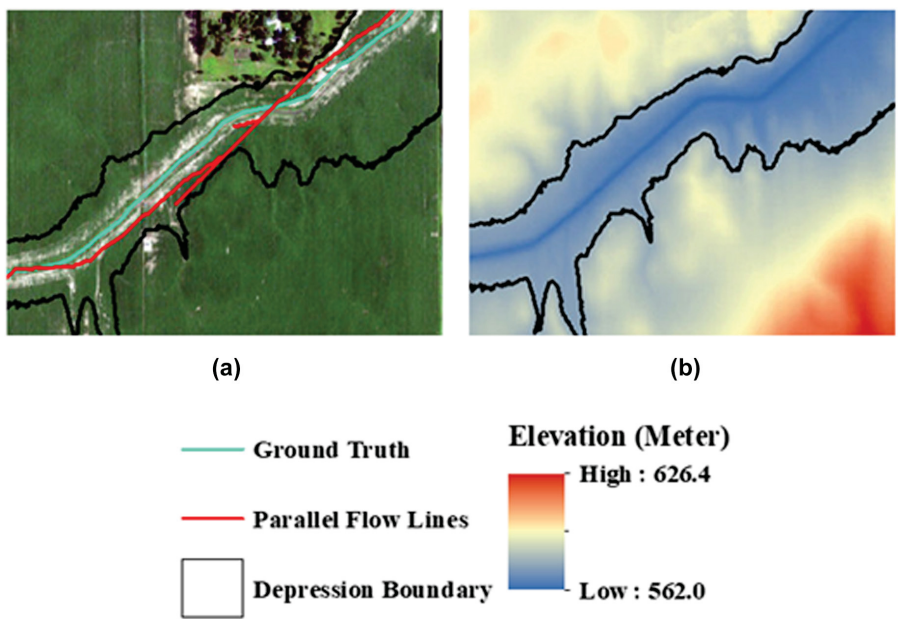


**FIGURE 13** An example of unrealistic flowlines in the flat area caused by filled depression. Black lines are the boundary of filled depression. (a) is the aerial photo where the cyan line is the ground truth and red line is the problematic parallel flow lines; (b) is the HRDEM in the same area where the original flow path is clear.

artificial drainage channels often create complicated connectivity patterns, which are difficult to identify or even verify in elevation-derived hydrography. The second type of omission errors (Figure 14b) are caused by missing canals that route water deliveries as a critical component of surface water irrigation infrastructures. To accurately determine these canals, additional information like the length and location of the canal, the direction of flow, and the historical canal network data in NHD should be taken into consideration (Terziotti & Archuleta, 2020). The third type is related to the headwater drainage channels that convey intermittent flows instead of perennial flows (Figure 14c). The challenge in generating these drainage ways caused by the difficulty in determining the headwater of a stream using the HRDEM and a fixed FAT, which can only approximate the representations of these drainageways (Terziotti & Archuleta, 2020). Ortho-imagery does not assist in the correction of these errors, as these drainageways are typically either less visible or lack clearly defined channels or banks. Therefore, in addition to the HRDEM, further field investigation may be needed to confirm these drainage channels.

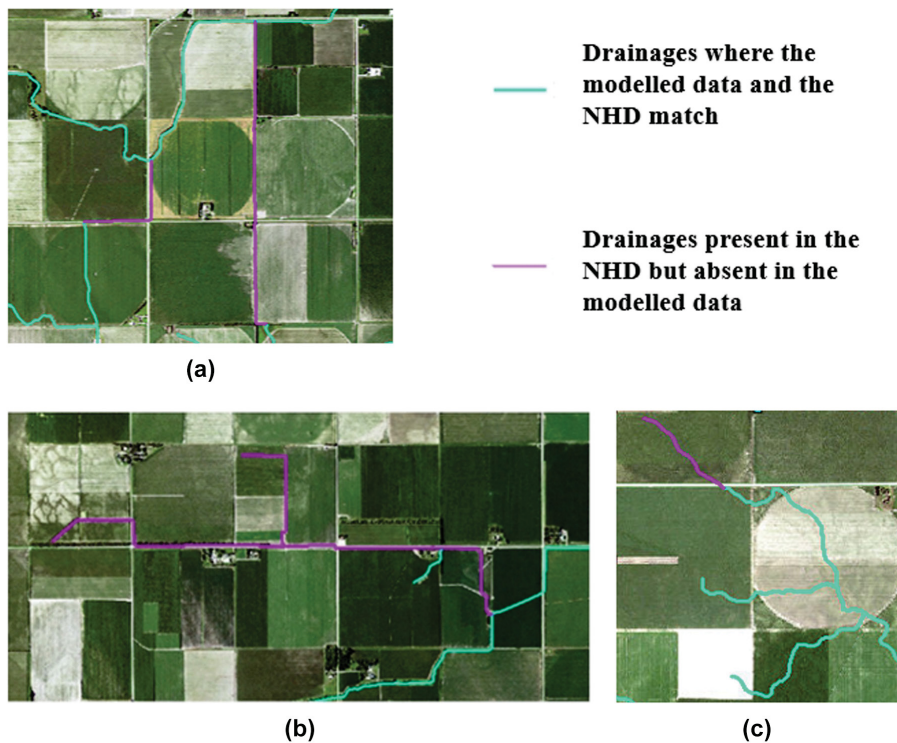


**FIGURE 14** Three types of omission errors. (a) The canals (purple lines) provided by NHD which connect two drainage networks (cyan lines). (b) Canal features (purple lines) that extend existing canal networks (cyan lines). (c) Representations of drainage channels (cyan lines) which did not capture the headwater (purple lines).

## 5.2 | Comparison between flowlines with and without DBP

To assess the improvement of generated flowlines associated with the removal of flow barriers, the flow accumulation method was applied to the original HRDEM without HRDEM excavation. In a comparison of error distribution maps before and after HRDEM excavation (Figures 8–11), the flow barriers were found to be responsible for the increases in commission errors and omission errors. Figure 15 is an example that shows the influence of a drainage structure, in which a drainage passing through the road was intercepted by road embankment. This 'digital dam' diverts the original flowpath to a more distant crossing location, contributing to new commission errors (red lines in Figure 15) and omission errors (yellow lines in Figure 15). The results in Tables 2 and 3 also prove that combining the drainage crossing lines with HRDEM can improve the elevation-derived hydrography. The CLC increased by 6.52% with combination of drainage crossing lines, meanwhile the commission errors and omission errors decreased by 2.77% and 3.75% respectively. This result is also consistent with the results from Li et al. (2013) and Bhadra et al. (2021). To resolve the flow barriers commonly present in the HRDEMs, new GeoAI models are being actively developed for the classification and detection of drainage barriers (Jalalipour et al., 2023; Wu et al., 2023; Zhang et al., 2023).

## 5.3 | Influence of different algorithms on flowlines derived by the excavated HRDEM

Based on the calculated CLC metric, we found that D-Infinity flowlines are similar to the D8 flowlines derived from the excavated HRDEM. The CLC for D8 and D-Infinity flowlines is 98.45%, which means that the similarity between these two flowlines is up to 98%. This similarity is also confirmed by Bhadra and his group (Bhadra et al., 2021), who also found that, after HRDEM excavation, D-Infinity and D8 flow direction was very similar for 1-meter HRDEM. Thus, we only focused on the D8-derived flowlines in this section.

## 5.4 | Uncertainties and future research

As aforementioned, unrealistic flow patterns in flat regions cause commission errors in hydrography network extraction. These flat regions may occur naturally or artificially arising from depression filling in DEM preprocessing. As elevation-derived flow direction relies on elevation differences, the accuracy of accumulated flowlines in flat areas is commonly low due to the lack of topographic variations (Liao et al., 2023). The

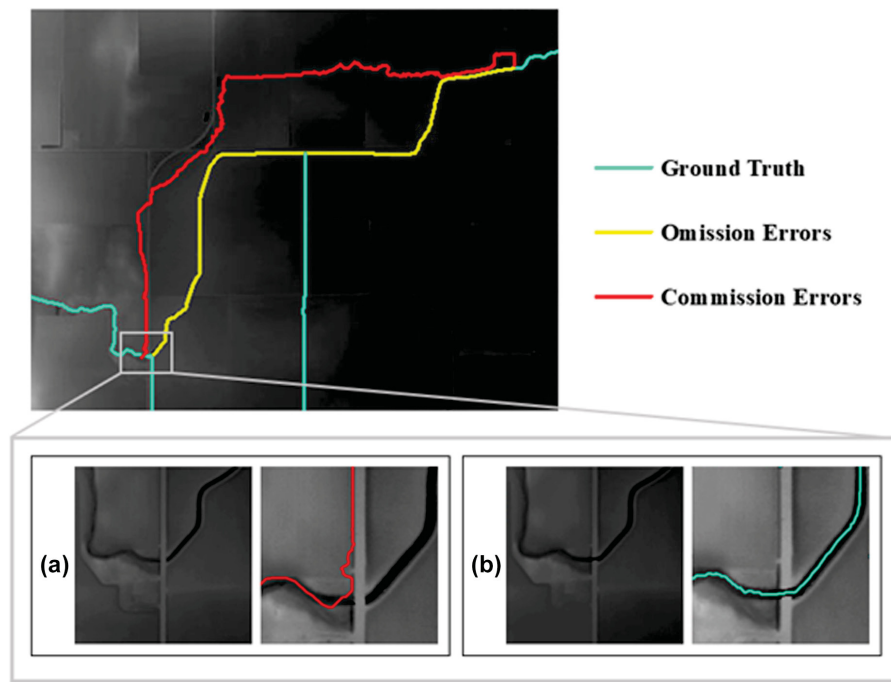


**FIGURE 15** An example of the influence of drainage structure on accumulated flowlines. In the upper graph, cyan lines represent the ground truth. The yellow lines are omission errors, and the red lines are commission errors caused by drainage structure. In the lower graph, (a) is the flowline derived from HRDEM without excavation, while (b) is the flowline derived from the excavated HRDEM.



**FIGURE 16** Elevation-derived flowlines (red lines) and flowlines from NHD (cyan lines) in Long Lake-Sutter Basin watershed, CA.

extraction of flow direction is confounded in flat areas to produce problematic parallel flow lines, and calculations also tend to be time-consuming. For those large depressions which are inhabited and don't accumulate water due to the disturbance of human activities, the situation could be too complex to delineate the correct flowpath based on elevation. Figure 16 shows an example of inhabited depressions, the Long Lake-Sutter Basin watershed in CA. After depression filling processing, the elevation-derived flowlines (red lines) are unrealistic parallels, while the flowpath should be controlled by artificial drainage channels (cyan lines) according to NHD. This example shows that the omission errors caused by complex artificial canal networks and commission errors caused by unrealistic parallels in the flat areas may be resolved using methods other than flow accumulation (for example, spatial segmentation by Xu et al., 2021). In these places, artificial drainage channels emerge as the predominant hydrographic features.

Although several flow-routing algorithms have been developed (Barnes et al., 2014b; Garbrecht & Martz, 1997; Jana et al., 2007; Tribe, 1992), it is still challenging to extract accurate flow directions for flat regions in DEMs (Zhang et al., 2017). For example, DBP in a HRDEM requires reference drainage flowlines in the flat areas, which are usually unavailable.

To address these limitations, spatial segmentation models like the U-net model may serve as a potential alternative solution. The U-net model could work with very few training images and yields more precise segmentations (Ronneberger et al., 2015). For hydrologic flowlines extraction, U-net could overcome the difficulties that are caused by spatial heterogeneity of surface water features, ensuring adequate connectivity of results by taking both the global and local information into consideration. Xu et al. (2021) developed an attention U-net model for fine-scale flowline detection by taking advantage of high-accuracy LiDAR data. The image was segmented based on the binary classification of stream and non-stream pixels. The results indicated that the attention U-net model could provide flowlines with better smoothness and connectivity. Thus, by using factors derived by HRDEM and corrected NHD "ground truth" as inputs, the U-net model could be a promising tool for our further research, which may conquer the challenge of flowlines delineation in flat areas.

## 6 | CONCLUSIONS

Fine-scale stream flowlines are crucial for managing small local basins and tributaries, yet they are often unavailable or unreliable. A key challenge in developing accurate fine-scale flowline data is the presence of flow barriers in HRDEMs, particularly at stream-road crossings, which can lead to incorrect flow patterns. By processing drainage barriers in HRDEMs, we created a flowlines dataset at a finer scale than the existing NHD and evaluated its quality. The unique contribution of this study is to develop a method and metrics for evaluating the effects of flow barrier processing on the accuracy of the modeled flowlines using HRDEMs. This evaluation also includes a comparative analysis of different flow delineation methods. The results suggest that:

1. The similarity of simulated flowlines with D8 and D-infinity algorithms is in a high degree, approximately 98%.
2. The commission errors are mainly associated with the presence of flow accumulation using a fixed FAT and unrealistic flowline artifacts occurring in large depressions, resulting in the divergence between the simulated flowlines and ground truth (corrected NHD) at a finer scale.
3. The omission errors primarily involve missing canals connecting natural drainage lines, missing irrigation canals that are crucial for delivering water, and challenges in identifying intermittent headwater drainage channels, resulting in discrepancies between simulated flowlines and the actual hydrography at a finer scale.
4. Processing flow barriers on HRDEMs can substantially improve the quality of hydrography mapping at fine scales.

### AUTHOR CONTRIBUTIONS

**Di Wu:** Formal analysis; investigation; methodology; visualization; writing – original draft. **Ruopu Li:** Conceptualization; funding acquisition; methodology; project administration; resources; supervision; writing – review and editing. **Michael Edidem:** Data curation. **Guangxing Wang:** Investigation.

### ACKNOWLEDGMENTS

This work was supported by a grant awarded by the National Science Foundation (1951741). We thank Claire Talbert for her contribution to data collection.

### CONFLICT OF INTEREST STATEMENT

The authors declare no conflict of interest.

### DATA AVAILABILITY STATEMENT

The data that support the findings of this study are available from the corresponding author upon request.

### REFERENCES

Anderson-Tarver, C., B.P. Buttenfield, L.V. Stanislawski, and J.M. Koontz. 2011. "Automated Delineation of Stream Centerlines for the USGS National Hydrography Dataset." In *Advances in Cartography and GIScience*, Vol 1, edited by A. Ruas, 409–23. Berlin, Heidelberg: Springer.

Anderson-Tarver, C., M. Gleason, B. Buttenfield, and L. Stanislawski. 2012. "Automated Centerline Delineation to Enrich the National Hydrography Dataset." In *International Conference on Geographic Information Science*, edited by S. Shekhar, 15–28. Berlin, Heidelberg: Springer.

Archuleta, C.A., and S. Terziotti. 2020. *Elevation-Derived Hydrography—Representation, Extraction, Attribution, and Delineation Rules* (No. 11-B12). Reston, VA: US Geological Survey.

Aristizabal, F., L.E. Grimley, J. Bales, D. Tijerina, T. Flowers, and E.P. Clark. 2018. *National Water Centers Innovators Program Summer Institute Report* 140. Arlington, MA: Consortium of Universities for the Advancement of Hydrologic Science, Inc. Technical Report No. 15.

Barber, C.P., and A. Shortridge. 2005. "Lidar Elevation Data for Surface Hydrologic Modeling: Resolution and Representation Issues." *Cartography and Geographic Information Science* 32(4): 401–10.

Barnes, R., C. Lehman, and D. Mulla. 2014a. "Priority-Flood: An Optimal Depression-Filling and Watershed-Labeling Algorithm for Digital Elevation Models." *Computers & Geosciences* 62: 117–27.

Barnes, R., C. Lehman, and D. Mulla. 2014b. "An Efficient Assignment of Drainage Direction over Flat Surfaces in Raster Digital Elevation Models." *Computers & Geosciences* 62: 128–35.

Bhadra, S., R. Li, D. Wu, G. Wang, and B. Rekabdar. 2021. "Assessing the Impacts of Anthropogenic Drainage Structures on Hydrologic Connectivity Using High-Resolution Digital Elevation Models." *Transactions in GIS* 25(5): 2596–611.

Buttenfield, B.P., L.V. Stanislawski, and C.A. Brewer. 2011. "A Comparison of Star and Ladder Generalization Strategies for Intermediate Scale Processing of USGS National Hydrography Dataset." In *Proceedings of 14th ICA/ISPRS Workshop on Generalisation and Multiple Representation*, edited by D. Burghardt and M. Sester. Paris, France: ICA Commission on Generalisation and Multiple Representation & the ISPRS Commission II/2 Working Group on Multiscale Representation of Spatial Data.

Carrivick, J.L., V. Manville, A. Graettinger, and S.J. Cronin. 2010. "Coupled Fluid Dynamics-Sediment Transport Modelling of a Crater Lake Break-out Lahar: Mt. Ruapehu, New Zealand." *Journal of Hydrology* 388(3–4): 399–413.

Evenson, G.R., H.E. Golden, C.R. Lane, D.L. McLaughlin, and E. D'Amico. 2018. "Depressional Wetlands Affect Watershed Hydrological, Biogeochemical, and Ecological Functions." *Ecological Applications* 28(4): 953–66.

Fekete, B.M., C.J. Vörösmarty, and R.B. Lammers. 2001. "Scaling Gridded River Networks for Macroscale Hydrology: Development, Analysis, and Control of Error." *Water Resources Research* 37(7): 1955–67.

Fesenmyer, K.A., S.J. Wenger, D.S. Leigh, and H.M. Neville. 2021. "Large Portion of USA Streams Lose Protection With New Interpretation of Clean Water Act." *Freshwater Science* 40(1): 252–8.

Figary, S., N. Detenbeck, and C. O'Donnell. 2021. "Guiding Riparian Management in a Transboundary Watershed through High Resolution Spatial Statistical Network Models." *Journal of Environmental Management* 278: 111585.

Garbrecht, J., and L.W. Martz. 1997. "The Assignment of Drainage Direction Over Flat Surfaces in Raster Digital Elevation Models." *Journal of Hydrology* 193(1–4): 204–13.

Heathcote, I.W. 2009. *Integrated Watershed Management: Principles and Practice*, 2nd ed. Hoboken, NJ: Wiley.

Hellweger, F. 1997, January 10. "Agree-DEM Surface Reconditioning System." April 25, 2021. <http://www.ce.utexas.edu/prof/maidment/gishydro/ferdi/research/agree/agree.html>.

Hout, R., V. Maleval, G. Mahe, E. Rouvellac, R. Crouzeviale, and F. Cerbelaud. 2020. "UAV and LiDAR Data in the Service of Bank Gully Erosion Measurement in Rambla de Algeciras Lakeshore." *Watermark* 12(10): 2748.

Huang, J., and E.A. Frimpong. 2016. "Modifying the United States National Hydrography Dataset to Improve Data Quality for Ecological Models." *Ecological Informatics* 32: 7–11.

Jalalipour, S., S. Ayyalasomayajula, H. Damrah, J. Lin, B. Rekabdar, and R. Li. 2023. "Deep Learning-Based Spatial Detection of Drainage Structures Using Advanced Object Detection Methods." In *2023 International Conference on Transdisciplinary AI 8*. Laguna Hills, CA: IEEE.

James, L.A., M.E. Hodgson, S. Ghoshal, and M.M. Latiolais. 2012. "Geomorphic Change Detection Using Historic Maps and DEM Differencing: The Temporal Dimension of Geospatial Analysis." *Geomorphology* 137(1): 181–98.

Jana, R., T.V. Reshmaidevi, P.S. Arun, and T.I. Eldho. 2007. "An Enhanced Technique in Construction of the Discrete Drainage Network from Low-Resolution Spatial Database." *Computers & Geosciences* 33(6): 717–27.

Jenkins, R.B., and P.S. Frazier. 2010. "High-Resolution Remote Sensing of Upland Swamp Boundaries and Vegetation for Baseline Mapping and Monitoring." *Wetlands* 30(3): 531–40.

Jenson, S.K., and J.O. Domingue. 1988. "Extracting Topographic Structure from Digital Elevation Data for Geographic Information System Analysis." *Photogrammetric Engineering and Remote Sensing* 54(11): 1593–600.

Lang, M., O. McDonough, G. McCarty, R. Oesterling, and B. Wilen. 2012. "Enhanced Detection of Wetland-Stream Connectivity Using LiDAR." *Wetlands* 32(3): 461–73.

Li, J., and D.W. Wong. 2010. "Effects of DEM Sources on Hydrologic Applications." *Computers, Environment and Urban Systems* 34(3): 251–61.

Li, R., Z. Tang, X. Li, and J. Winter. 2013. "Drainage Structure Datasets and Effects on LiDAR-Derived Surface Flow Modeling." *ISPRS International Journal of Geo-Information* 2(4): 1136–52.

Liao, C., T. Zhou, D. Xu, M.G. Cooper, D. Engwirda, H.Y. Li, and L.R. Leung. 2023. "Topological Relationship-Based Flow Direction Modeling: Mesh-Independent River Networks Representation." *Journal of Advances in Modeling Earth Systems* 15(2): e2022MS003089.

Lin, W.T., W.C. Chou, C.Y. Lin, P.H. Huang, and J.S. Tsai. 2006. "Automated Suitable Drainage Network Extraction from Digital Elevation Models in Taiwan's Upstream Watersheds." *Hydrological Processes: An International Journal* 20(2): 289–306.

Lindsay, J.B. 2016. "The Practice of DEM Stream Burning Revisited." *Earth Surface Processes and Landforms* 41(5): 658–68.

Lindsay, J.B., and K. Dhun. 2015. "Modelling Surface Drainage Patterns in Altered Landscapes Using LiDAR." *International Journal of Geographical Information Science* 29(3): 397–411.

McKay, L., T. Bondelid, T. Dewald, J. Johnston, R. Moore, and A. Rea. 2014. *NHDPlus Version 2: User Guide*. U.S. Environmental Protection Agency.

Mukhopadhyay, S., A. Sankarasubramanian, and C. Awasthi. 2020. "Developing the Hydrological Dependency Structure Between Streamgage and Reservoir Networks." *Scientific Data* 7(1): 1–9.

O'Callaghan, J.F., and D.M. Mark. 1984. "The Extraction of Drainage Networks from Digital Elevation Data." *Computer Vision, Graphics, and Image Processing* 28(3): 323–44.

Ozulu, I.M., and T. Gökgöz. 2018. "Examining the Stream Threshold Approaches Used in Hydrologic Analysis." *ISPRS International Journal of Geo-Information* 7(6): 201.

Poppenga, S.K., D.B. Gesch, and B.B. Worstell. 2013. "Hydrography Change Detection: The Usefulness of Surface Channels Derived from LiDAR DEMs for Updating Mapped Hydrography." *Journal of the American Water Resources Association* 49(2): 371–89.

Qin, C., A.X. Zhu, T. Pei, B. Li, C. Zhou, and L. Yang. 2007. "An Adaptive Approach to Selecting a Flow-Partition Exponent for a Multiple-Flow-Direction Algorithm." *International Journal of Geographical Information Science* 21(4): 443–58.

Quinn, P.F.B.J., K. Beven, P. Chevallier, and O. Planchon. 1991. "The Prediction of Hillslope Flow Paths for Distributed Hydrological Modelling Using Digital Terrain Models." *Hydrological Processes* 5(1): 59–79.

Ronneberger, O., P. Fischer, and T. Brox. 2015. "U-Net: Convolutional Networks for Biomedical Image Segmentation." In *Medical Image Computing and Computer-Assisted Intervention–MICCAI 2015: 18th International Conference, Munich, Germany, October 5–9, 2015, Proceedings, Part III 18*, edited by N. Navab, J. Hornegger, W. Wells, and A. Frangi, 234–41. Cham, Switzerland: Springer International Publishing.

Saunders, W. 2000. *Preparation of DEMs for Use in Environmental Modeling Analysis*. *Hydrologic and Hydraulic Modeling Support* 29–51. Redlands, CA: ESRI.

Simley, J. 2008. "Applying the National Hydrography Dataset." *Water Resources Impact* 10(1): 5–8.

Sofia, G., G.D. Fontana, and P. Tarolli. 2014. "High-Resolution Topography and Anthropogenic Feature Extraction: Testing Geomorphometric Parameters in Floodplains." *Hydrological Processes* 28(4): 2046–61.

Stanislawski, L.V. 2009. "Feature Pruning by Upstream Drainage Area to Support Automated Generalization of the United States National Hydrography Dataset." *Computers, Environment and Urban Systems* 33(5): 325–33.

Steinke, R.C., and F.L. Ogden. 2013, December. "Evaluating TauDEM Delineated Stream Networks Against the National Hydrography Dataset." AGU Fall Meeting Abstracts (Vol. 2013, pp. H23E-1310).

Strager, M.P. 2019. "Protecting Surface Water Drinking Supplies in WV With Zones of Critical Concern." In *Geospatial Information System Use in Public Organizations: How and Why GIS Should Be Used in the Public Sector*, Vol 112, edited by N. Valcik. New York, NY: Routledge.

Tarboton, D.G. 1997. "A New Method for the Determination of Flow Directions and Upslope Areas in Grid Digital Elevation Models." *Water Resources Research* 33(2): 309–19.

Tarboton, D.G., and I.N. Mohammed. 2013. *TauDEM 5.1 Quick Start Guide to Using the TauDEM ArcGIS Toolbox*. Logan, UT: Utah State University.

Terziotti, S., and C.A. Archuleta. 2020. *Elevation-Derived Hydrography Acquisition Specifications* (No. 11-B11). Reston, VA: U.S. Geological Survey.

Thomas, K.A., M.L. McTeague, L. Ogden, M.L. Floyd, K. Schulz, B.A. Friesen, T.S. Fancher, R.G. Waltermire, and A. Cully. 2009. *Vegetation Classification and Distribution Mapping Report: Mesa Verde National Park* (No. NPS/SCPN/NRR-2009/112). Fort Collins, CO: National Park Service.

Thompson, P.A., S.A. Welsh, M.P. Strager, and A.A. Rizzo. 2018. "A Multiscale Investigation of Habitat Use and Within-River Distribution of Sympatric Sand Darter Species." *Journal of Geospatial Applications in Natural Resources* 2(1): 1.

Tribe, A. 1992. "Automated Recognition of Valley Lines and Drainage Networks from Grid Digital Elevation Models: A Review and a New Method." *Journal of Hydrology* 139(1–4): 263–93.

Wang, J., L. Li, Z. Hao, and J.J. Gourley. 2011. "Stream Guiding Algorithm for Deriving Flow Direction from DEM and Location of Main Streams." *IAHS AISH Publication* 346: 198–206.

Wilmer, J.M. 2010. Application of the Radical Law in Generalization of National Hydrography Data for Multiscale Mapping. Master's thesis, The Pennsylvania State University. University Park, PA.

Wu, D., R. Li, C. Talbert, M. Edidem, B. Rekabdar, and G. Wang. 2023. "Classification of Drainage Crossings on High-Resolution Digital Elevation Models: A Deep Learning Approach." *GIScience & Remote Sensing* 60: 1. <https://doi.org/10.1080/15481603.2023.2230706>.

Xu, Z., S. Wang, L.V. Stanislawski, Z. Jiang, N. Jaroenchai, A.M. Sainju, E. Shavers, et al. 2021. "An Attention U-Net Model for Detection of Fine-Scale Hydrologic Streamlines." *Environmental Modelling & Software* 140: 104992.

Yang, J., and X. Chu. 2013. "Effects of DEM Resolution on Surface Depression Properties and Hydrologic Connectivity." *Journal of Hydrologic Engineering* 18(9): 1157–69.

Yang, T.H., Y.C. Chen, Y.C. Chang, S.C. Yang, and J.Y. Ho. 2015. "Comparison of Different Grid Cell Ordering Approaches in a Simplified Inundation Model." *Watermark* 7(2): 438–54.

Zhang, H., H.A. Loáiciga, L. Feng, J. He, and Q. Du. 2021. "Setting the Flow Accumulation Threshold Based on Environmental and Morphologic Features to Extract River Networks From Digital Elevation Models." *ISPRS International Journal of Geo-Information* 10(3): 186.

Zhang, H., Z. Yao, Q. Yang, S. Li, J.E. Baartman, L. Gai, M. Yao, X. Yang, C.J. Ritsema, and V. Geissen. 2017. "An Integrated Algorithm to Evaluate Flow Direction and Flow Accumulation in Flat Regions of Hydrologically Corrected DEMs." *Catena* 151: 174–81.

Zhang, Y., D. Pandey, D. Wu, T. Kundu, R. Li, and T. Shu. 2023. "Accuracy-Constrained Efficiency Optimization and GPU Profiling of CNN Inference for Detecting Drainage Crossing Locations." In *The International Conference for High Performance Computing, Networking, Storage, and Analysis (SC23)*, 1780–8. Denver, CO: IEEE Computer Society. <https://doi.org/10.1145/3624062.3624260>.

**How to cite this article:** Wu, Di, Ruopu Li, Michael Edidem and Guangxing Wang. 2024. "Enhancing Hydrologic LiDAR Digital Elevation Models: Bridging Hydrographic Gaps at Fine Scales." *JAWRA Journal of the American Water Resources Association* 60(6): 1253–1269.

<https://doi.org/10.1111/1752-1688.13239>.